



Flux weighted average cross section measurement of some technically important radioisotopes from natural cadmium induced by bremsstrahlung



Muhammad Nadeem^{ab}, Muhammad Shahid^{bc}, Guinyun Kim^b, Iftikhar Alam^a, Muhammad Asghar^a, M. Arshad^a

Abstract

We measured the flux-weighted average photo-neutron cross-sections and isomeric yield ratios of cadmium isotopes produced from $^{nat}\text{Cd}(\gamma, xn; x=1-6)$ reactions and silver isotopes produced from $^{nat}\text{Cd}(\gamma, pxn)$ with the bremsstrahlung end-point energies of 50-60-MeV at the Pohang Accelerator Laboratory (PAL), Korea. The photonuclear yields of the important isotopes from the reactions are also measured. The present measured values were compared with evaluated nuclear data based on TALYS-1.95 and Empire 3.2.2 Malta together with literature values and found mostly in good agreement.

Keywords: Geant4 Monte Carlo simulation tool, off-line γ -ray spectrometric technique, $^{nat}\text{Cd}(\gamma, xpxn)$ nuclear reactions, EMPIRE-3.2, TALYS-1.95, EXFORE nuclear data library.

I. Introduction

The photo-nuclear reactions such as $(\gamma, xn; x=1-6)$ within GDR and QD region gives important parameters of a nuclear reaction. The flux weighted photo-neutron cross-section via the $^{nat}\text{Cd}(\gamma, xn)^{115g,m,111m,109,107}\text{Cd}$ and $^{nat}\text{Cd}(\gamma, pxn)^{113g,112}\text{Ag}$ reactions are the first time measurement. The presently measured isomeric yield ratios (IYR) of $^{115m,g}\text{Cd}$ in the $^{nat}\text{Cd}(\gamma, xn)$ reactions provide information on nuclear reaction parameters in testing theoretical model as well as in various practical applications in science and technology. The photo-activation method and off-line γ -ray spectrometric technique is used.

II. Experimental Setup

The experiments were performed by using an electron linac at the Pohang Accelerator Laboratory (PAL) in Korea. The bremsstrahlung was generated when a pulsed electron beam hits a thin tungsten (W) foil with a size of 10.0 cm \times 10.0 cm and a thickness of 0.1 mm. The tungsten target was placed at a distance of 18.0 cm from the electron beam exit window. The sample was fixed on a stand at 12 cm from the W target, and 0 $^\circ$ relative to the electron beam direction. The bremsstrahlung spectrum was calculated with the GEANT 4 code at the position of the sample irradiation.



Fig. 1. Electron linac at Pohang Accelerator Laboratory (PAL).

$$\langle E^*(E_e) \rangle = \frac{\int_{E_{th}}^{E_e} N(E_e, E_\gamma) \sigma_R(E_\gamma) E_\gamma dE_\gamma}{\int_{E_{th}}^{E_e} N(E_e, E_\gamma) \sigma_R(E_\gamma) dE_\gamma}$$

- Electron energy: 50 ~ 60 MeV
- Repetition rate: < 15 Hz
- Pulse width: 2 μ s
- Peak beam current: 20 ~ 36 mA

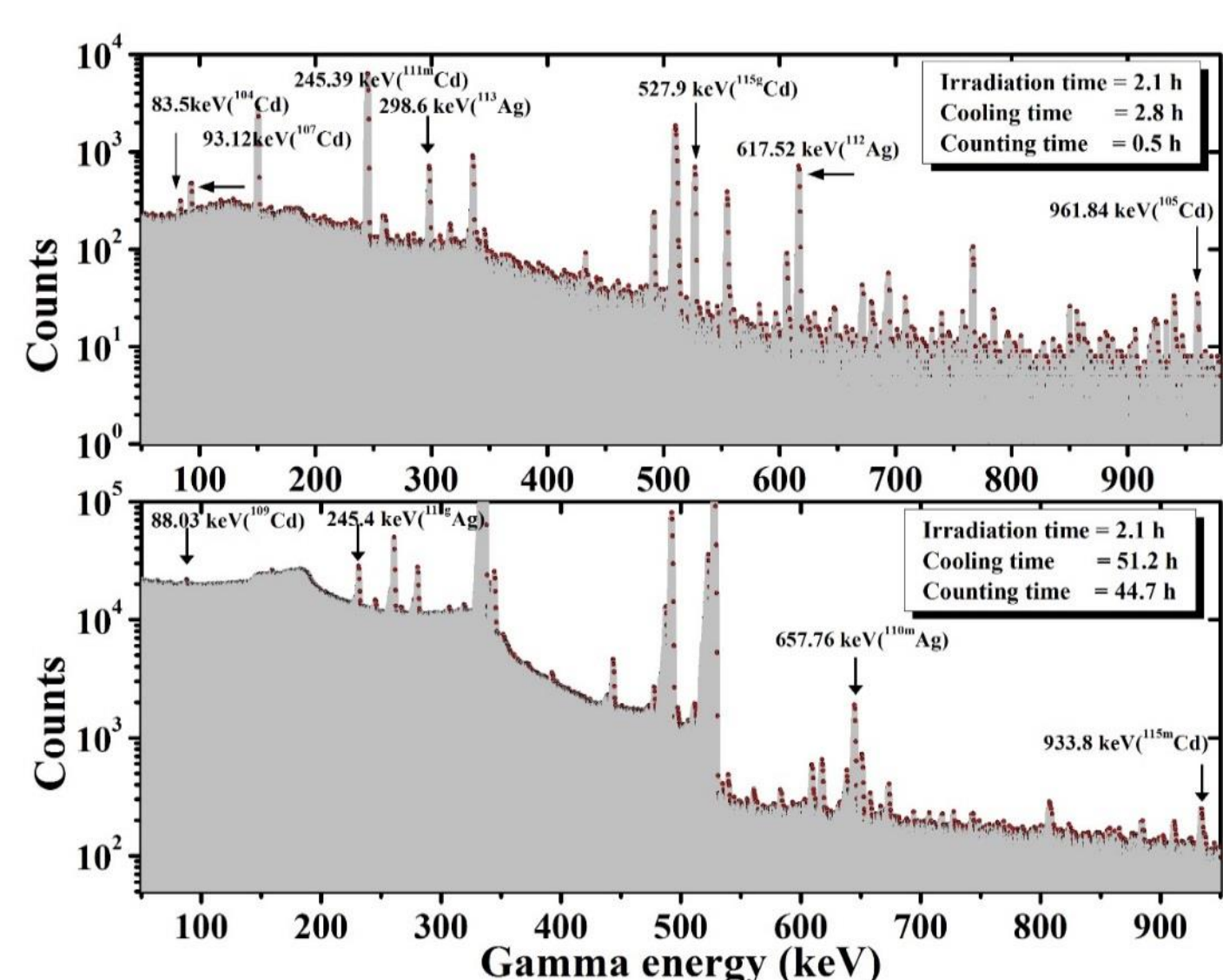


Fig. 2. Typical γ -ray spectra of natural cadmium reaction products

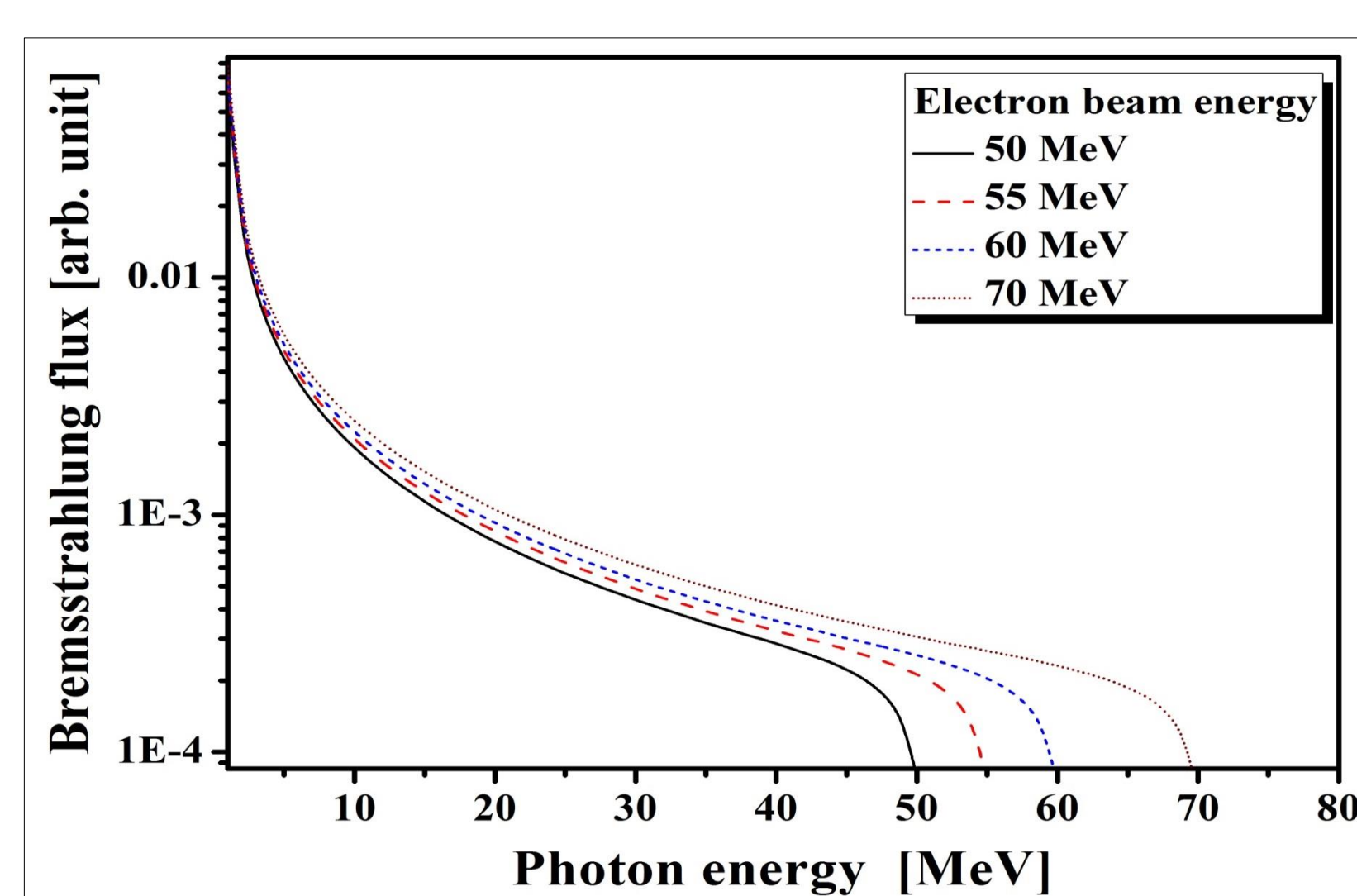


Fig. 3: Bremsstrahlung spectrum with Geant4 code

III. Data Analysis

Flux weighting factors :

Flux weighted factors (F_{wf})	E_{th} (MeV)	Bremsstrahlung end-point energy (MeV)	
		50	60
$^{nat}\text{Cd}(\gamma, n)^{115g}\text{Cd}$	8.70	0.934	0.941
$^{nat}\text{Cd}(\gamma, n)^{115m}\text{Cd}$	8.70	0.934	0.941
$^{nat}\text{Cd}(\gamma, xn)^{111m}\text{Cd}$	39.82	0.774	0.774
$^{nat}\text{Cd}(\gamma, xn)^{109}\text{Cd}$	10.33	0.753	0.765
$^{nat}\text{Cd}(\gamma, xn)^{107}\text{Cd}$	9.92	0.629	0.602
$^{nat}\text{Cd}(\gamma, pxn)^{113g}\text{Ag}$	10.28	0.761	0.806
$^{nat}\text{Cd}(\gamma, pxn)^{112}\text{Ag}$	9.75	0.565	0.576

Excitation Energy

$$\langle E^*(E_e) \rangle = \frac{\int_{E_{th}}^{E_e} \phi(E) \sigma_R(E) E dE}{\int_{E_{th}}^{E_e} \phi(E) \sigma_R(E) dE}$$

Yields

$$Y = \int_{E_{th}}^{E_e} C_i \sigma_i(E) \phi_i(E) dE \left/ \sum C_i \int_{E_{th}}^{E_e} \sigma_i(E) \phi_i(E) dE \right.$$

$$\sigma_R(E) = \frac{N_{obs} \left(\frac{CL}{IT} \right) \lambda}{n f \phi_n I_\gamma \epsilon (1 - e^{-\lambda T_i}) e^{-\lambda T_w} (1 - e^{-\lambda T_c})}$$

$- C_i$: Natural Abundance for ^{116}Cd (7.49%), ^{114}Cd (28.73%), ^{113}Cd (12.22%), ^{112}Cd (24.13%), ^{111}Cd (12.8%), ^{110}Cd (12.49%), ^{108}Cd (0.89%) and ^{106}Cd (1.25%)
 $- \sigma_i(E)$: Cross-Section calculated by TALYS/Empire codes
 $- \phi_i(E)$: Photon flux calculated by Geant4

^aBahawalpur Institute of Nuclear Medicine and Oncology (BINO), PAEC Bahawalpur.

^bDepartment of Physics, Kyungpook National University, Daegu 41566, South Korea.

^cPakistan Nuclear Regulatory Authority (PNRA), Islamabad.

IV. Results and discussion

Natural Cadmium

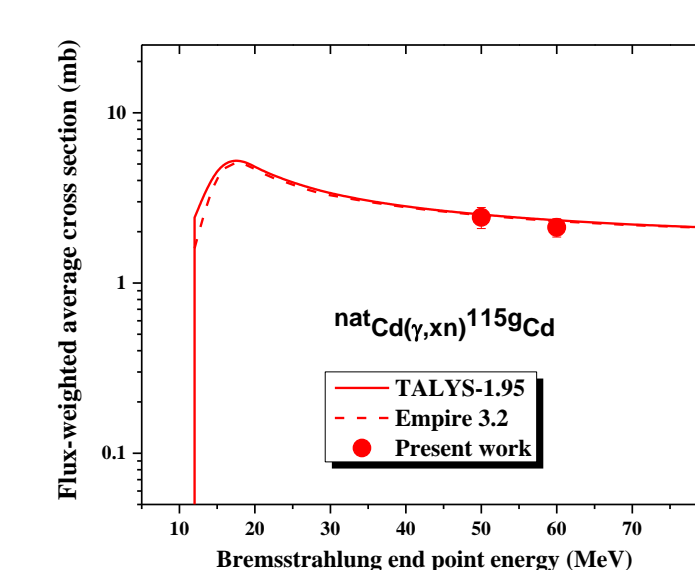


Fig. 4. Photo-neutron cross-section of $^{nat}\text{Cd}(\gamma, xn; x=1)$ ^{115g}Cd reactions for mono-energetic photon.

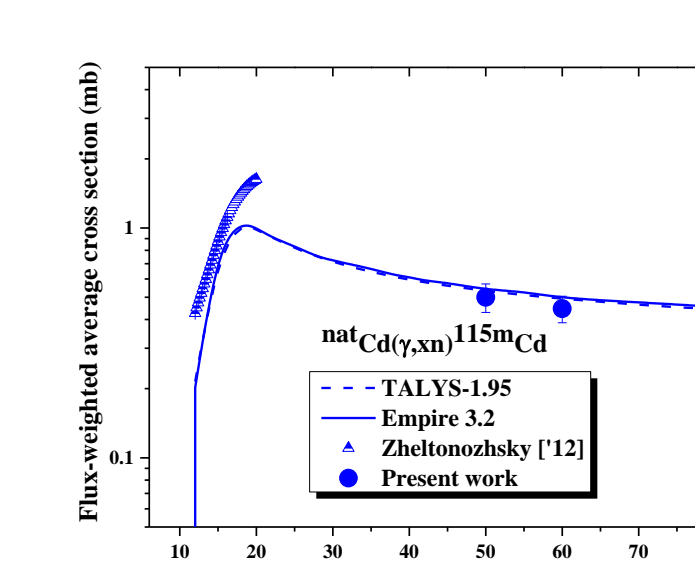


Fig. 5. Flux-weighted average cross-sections of the $^{nat}\text{Cd}(\gamma, xn)^{115m}\text{Cd}$ reactions with brems. end-point energy.

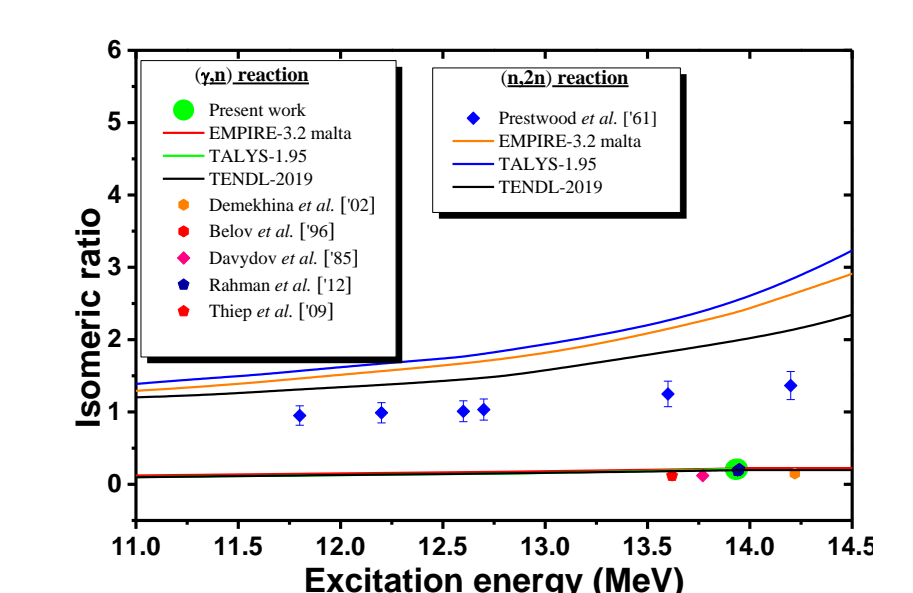


Fig. 6. The isomeric yield ratio ($IR=Y_m/Y_g$) of $^{115m,g}\text{Cd}$ as a function of excitation energy of the compound nucleus.

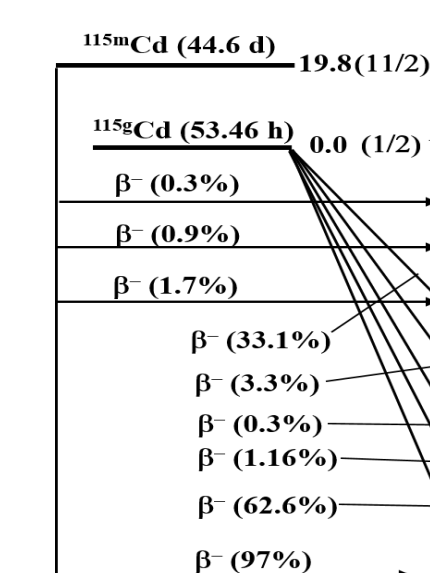


Fig. 7. Decay scheme of $^{nat}\text{Cd}(\gamma, xn; x=1)$ $^{115m,g}\text{Cd}$ reactions for mono-energetic photon.

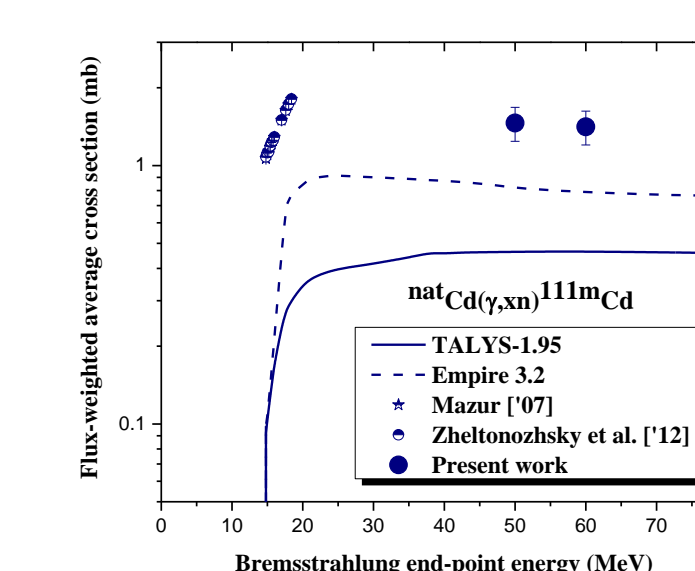


Fig. 8. Flux-weighted average cross-sections of the $^{nat}\text{Cd}(\gamma, xn)^{111m}\text{Cd}$ reactions with brems. end-point energy.

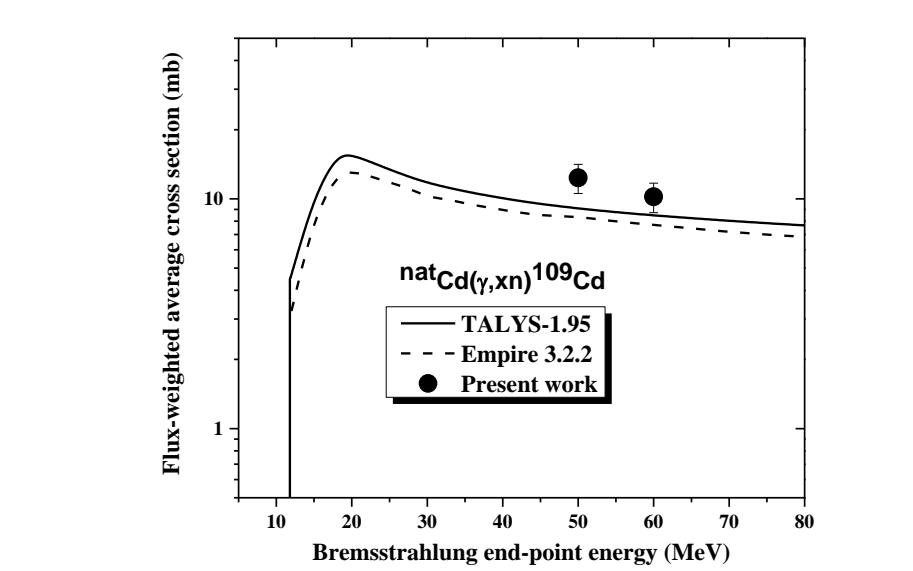


Fig. 9. Flux-weighted average cross-sections of the $^{nat}\text{Cd}(\gamma, xn)^{109}\text{Cd}$ reactions with brems. end-point energy.

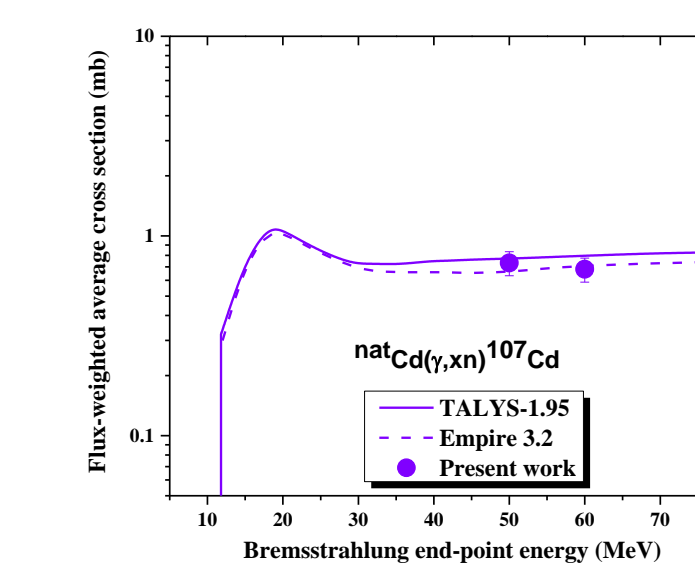


Fig. 10. Flux-weighted average cross-sections of the $^{nat}\text{Cd}(\gamma, xn)^{107}\text{Cd}$ reactions with brems. end-point energy.

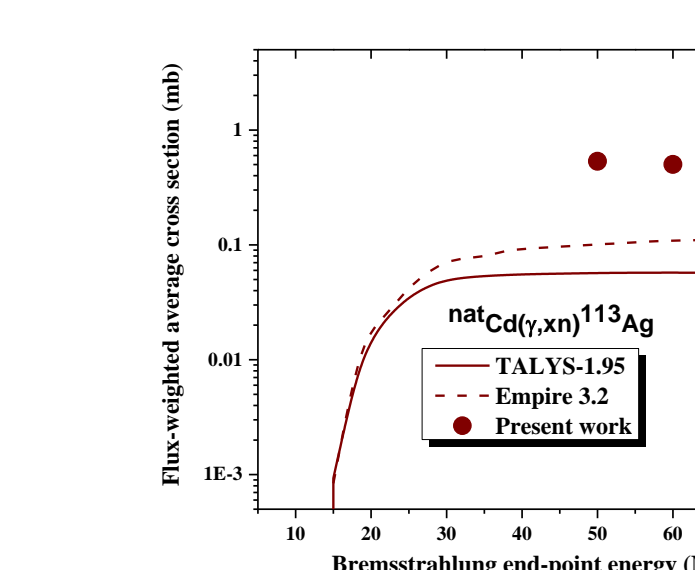


Fig. 11. Flux-weighted average cross-sections of the $^{nat}\text{Cd}(\gamma, xn)^{113g}\text{Ag}$ reactions with brems. end-point energy.

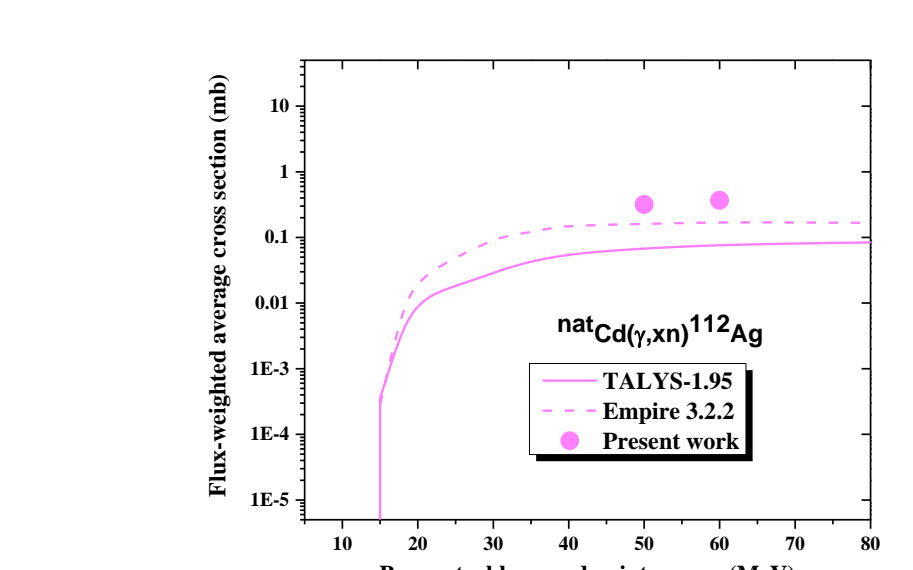


Fig. 12. Flux-weighted average cross-sections of the $^{nat}\text{Cd}(\gamma, xn)^{112}\text{Ag}$ reactions with brems. end-point energy.

Nuclear Reactions	Brems. end point energy, MeV	Experimental value of flux weighted average cross-section in mb	Theoretical values of $\langle \sigma \rangle$	
			TALYS 1.95	Empire 3.2.2 Malta
$^{nat}\text{Cd}(\gamma, n)^{115g}\text{Cd}$	50	2.432 ± 0.345	2.521	2.526
	60	2.123 ± 0.261	2.330	2.329
$^{nat}\text{Cd}(\gamma, n)^{115m}\text{Cd}$	50	0.5 ± 0.071	0.534	0.553
	60	0.446 ± 0.059	0.492	0.510
$^{nat}\text{Cd}(\gamma, xn)^{111m}\text{Cd}$	50	1.461 ± 0.219	0.458	0.811
	60	1.413 ± 0.212	0.449	0.785
$^{nat}\text{Cd}(\gamma, xn)^{109}\text{Cd}$	50	12.346 ± 1.786	9.082	8.381
	60	10.210 ± 1.501	8.466	7.724
$^{nat}\text{Cd}(\gamma, xn)^{107}\text{Cd}$	50	0.733 ± 0.101	0.788	0.656
	60	0.681 ± 0.094	0.834	0.711
$^{nat}\text{Cd}(\gamma, pxn)^{113g}\text{Ag}$	50	0.534 ± 0.075	0.057	0.108
	60	0.501 ± 0.061	0.057	0.110
$^{nat}\text{Cd}(\gamma, pxn)^{112}\text{Ag}$	50	0.318 ± 0.043	0.068	0.159
	60	0.367 ± 0.046	0.081	0.172

Photo-nuclear Yields [Bq/g.μAh]

Reaction	Isotope	Yields Y_γ [Bq/g.μAh]	
		Bremsstrahlung end-point energy	
		50 MeV	60 MeV
$^{nat}\text{Cd}(\gamma, n)^{115g}\text{Cd}$	^{115g}Cd	$(8.83 \pm 0.57) \cdot 10^6$	$(8.52 \pm 0.60) \cdot 10^7$
$^{nat}\text{Cd}(\gamma, n)^{115m}\text{Cd}$	^{115m}Cd	$(1.86 \pm 0.12) \cdot 10^6$	$(1.80 \pm 0.19) \cdot 10^7$
$^{nat}\text{Cd}(\gamma, xn)^{111m}\text{Cd}$	^{111m}Cd	$(4.48 \pm 0.28) \cdot 10^6$	$(8.99 \pm 0.61) \cdot 10^7$
$^{nat}\text{Cd}(\gamma, xn)^{109}\text{Cd}$	^{109}Cd	$(3.62 \pm 0.26) \cdot 10^7$	$(2.49 \pm 0.21) \cdot 10^8$
$^{nat}\text{Cd}(\gamma, xn)^{107}\text{Cd}$	^{107}Cd	$(1.71 \pm 0.12) \cdot 10^6$	$(1.73 \pm 0.12) \cdot 10^7$
$^{nat}\text{Cd}(\gamma, pxn)^{113g}\text{Ag}$	$^{113m,g}\text{Ag}$	$(1.58 \pm 0.11) \cdot 10^6$	$(1.67 \pm 0.11) \cdot 10^7$
$^{nat}\text{Cd}(\gamma, pxn)^{112}\text{Ag}$	^{112}Ag	$(7.0 \pm 0.41) \cdot 10^5$	$(8.74 \pm 0.53) \cdot 10^6$

Relative photo-nuclear yields of $^{115g,m,111m,109,107}\text{Cd}$ and $^{113g,112}\text{Ag}$ via (γ, n) with $^{197}\text{Au}(\gamma, n)^{196}\text{Au}$ reactions

V. Uncertainties

The overall uncertainty is the quadratic sum of both systematic and statistical errors. The total systematic error is about 15% to 16%. Statistical error was also ranges from 1% to 20%. The overall uncertainties for the reaction cross sections are in between 17% to 23%.

VI. Conclusion

We have experimentally determined and theoretically calculated and compared the flux-weighted average cross-sections of $^{nat}\text{Cd}(\gamma, xn)^{115g,m,111m,109,107}\text{Cd}$ and $^{nat}\text{Cd}(\gamma, pxn)^{113g,112}\text{Ag}$ and the isomeric yield ratios of $^{nat}\text{Cd}(\gamma, xn)^{115g,m}$ with the bremsstrahlung end-point energies of 50-60-MeV. In comparison with charge particle induced reactions and the following observations could be made. (i) The experimental and the theoretical reaction cross-sections increase from their respective threshold values to a certain bremsstrahlung energy, where the other reaction channel opens up. Thereafter, it decreases with increase of bremsstrahlung energy due to opening of other reaction channels. (ii) The IYR value of same increase with increase of projectile energy, which indicates the role of excitation energy. (iii) At the same excitation energy, the IR value of same reaction product in the charged particle induced reactions is higher than in the photon and neutron induced reactions, which indicate the role of input angular momentum. (iv) The photo-nuclear yields are also higher at higher photon energy.